MALAYSIAN JOURNAL OF SCIENCE
MJS
ISSN 1394 - 3065

2nd Euro-Asia Conference on CO_2 Capture and Utilization (EACCO2CU2022)

Special issue

Malaysian Journal of Science 43 (Special Issue 1): 50-57 (July 2024)

https://mjs.um.edu.my

IONIC LIQUIDS AS POTENTIAL CO-CATALYST FOR CO_2 ELECTROCHEMICAL REDUCTION

Sulafa Abdalmageed Saadaldeen Mohammed[1a,b], Wan Zaireen Nisa Yahya[2a,c*], Mohamad Azmi Bustam[3a,c] , Muzamil A.Hassan[4d], Asiah Nusaibah Masri[5e], Md Golam Kibria[6f]

Abstract: Carbon dioxide electrochemical reduction (CO_2ER) presents numerous advantages in mitigating greenhouse gas emissions by converting CO_2 into value-added chemicals and can be integrated with renewable energy sources such as solar and wind. Nevertheless, establishing an electrochemically stable catalytic system that can effectively decrease the overpotential while maintaining high current density and faradaic efficiency is challenging. The precise mechanisms causing the reactions and the specific functions of the electrode with electrolytes are still not fully understood. Hence, a significant increase in attention has been paid to using ionic liquids (ILs) as electrolytes for CO_2ER. This phenomenon is attributed to the unique capabilities of ILs to reduce overpotential, increase current density, and improve electrochemical stability. Therefore, this study evaluated the effect of incorporating ILs into electrolytes to comprehend the cation and anion influences on CO_2ER reactions. Linear sweep voltammetry (LSV) and chronoamperometry (CA) were employed to examine the reduction peaks and current density values for different electrolytes, respectively. Consequently, a 0.1 M NBu_4PF_6 acetonitrile solution containing 1-ethyl-3-methylimidazolium tetrafluoroborate [EMIM][BF_4] demonstrated a significantly lower onset potential of the reduction by 320 mV. A reduced CO_2ER efficiency involving ILs with long alkyl chains was also observed. Meanwhile, a novel hypothesis concerning molecular orbitals for the CO_2ER reaction mechanism was discussed. Overall, various performance variables (reduction stability, applied potential, and current density) of CO_2ER were improved using cations with short alkyl chains, anions with high highest occupied molecular orbital (HOMO) levels, and appropriate solvation media. These findings can serve as selection criteria to aid in choosing appropriate ionic liquids for CO_2 electrochemical reduction (CO_2ER).

Keywords: Ionic liquids, CO_2 conversion, electrochemical reduction, COSMO-RS, Turbomole

1. Introduction

Considering the progress of the global economy and society, the growing energy demand is a pressing issue that must be addressed. Despite the considerable advancements in green renewable energy sources (such as solar and wind energy), fossil fuels remain the dominant primary source (accounting for more than 80% of energy output) (Yang *et al*., 2008; Tian *et al*., 2022). Generally, fossil fuels release significant carbon dioxide (CO_2) into the atmosphere, causing its entrapment. Numerous environmental and climate change issues are then observed due to the disruption of the global carbon cycle. Higher sea levels and greenhouse effect intensification are two common examples caused by this phenomenon (Friedlingstein *et al*., 2014). Hence, the negative impacts necessitate a highly effective method for converting CO_2 into valuable compounds to lower the atmospheric CO_2 concentration. Several studies have addressed these issues by efficiently developing strategies to convert CO_2 into valuable carbon-based compounds. These approaches include thermal reduction (Shi *et al*., 2018), biotransformation (Karishma *et al*., 2024), photoelectrochemical (Bi *et al*., 2022), and electrochemical reduction (Gu *et al*., 2022).

The CO_2 electrochemical reduction (CO_2ER) system can produce numerous value-added products through CO_2 conversion, including methane (CH_4), ethylene (C_2H_4), carbon monoxide (CO), methanol (CH_3OH), formic acid (CH_2O_2), and ethanol (C_2H_5OH). Notably, the cathode material is the primary catalyst in the CO_2ER system. Multiple studies by Hori *et al*. also reported the effects of different metal catalysts on CO_2ER, such as Cu, Au, In, Sn, Pb, Zn, Ag, and Pd (Y. Hori *et al*., 1987; Y. Hori *et al*., 1994; Y. i. Hori, 2008). Consequently, Cu and its derivatives have been extensively researched as catalysts due to their unique capability to efficiently convert CO_2 into several higher products, surpassing the production of only CO. These reactions occur at ambient conditions and exhibit high current efficiencies. Nevertheless, ILs have garnered significant interest as an electrolyte for CO_2ER due to their distinctive characteristics,

Authors information:
[a]Chemical Engineering Department, Universiti Teknologi PETRONAS, 32610 Seri Iskandar, Perak, MALAYSIA.
[b]Department of Energy, Aalborg University, 9220 Aalborg, Denmark. E-mail: sasm@energy.aau.dk[1]
[c]Centre for Research in Ionic Liquid, Universiti Teknologi PETRONAS, 32610 Seri Iskandar, Perak, MALAYSIA. E-mail: azmibustam@utp.edu.my[3]
[d]Centre for Biofuel and Biochemical Research, Institute for Sustainable Building, Universiti Teknologi PETRONAS, 32610 Seri Iskandar, Perak, MALAYSIA. E-mail: muzamil.hassan@utp.edu.my[4]
[e]Energy Engineering Department, School of Chemical and Energy Engineering, Faculty of Engineering, Universiti Teknologi Malaysia, 81310 Skudai, Johor, MALAYSIA. E-mail: nusaibah@utm.my[5]
[f]Chemical and Petroleum Engineering, University of Calgary, 2500 University Drive, NW, Calgary, Alberta T2N 1N4, CANADA. E-mail: md.kibria@ucalgary.ca[6]

*Corresponding Author: zaireen.yahya@utp.edu.my

Received: February 7, 2024
Accepted: May 7, 2024
Published: July 31, 2024

DOI: https://doi.org/10.22452/mjs.vol43sp1.9
Malaysian Journal of Science 43 (Special Issue 1): 50-57 (July 2024)

including excellent thermal and chemical stability, good CO_2 solubility, and the capacity to reduce the applied potential (Carlesi *et al*., 2014).

The cations of the ILs have been reported as the primary active component influencing catalytic performance and have garnered significant interest (Lau *et al*., 2016). Specifically, imidazolium-based ILs have demonstrated substantial potential and can be categorised into two divergent mechanisms. Firstly, the ILs and CO_2 form a covalent bonding by carboxylic adduct formation, or that hydride is transmitted. Secondly, the ILs and CO_2 form non-covalent interactions, such as stabilising complexes through alterations in the localised CO_2 environment or hydrogen bonding (Vasilyev *et al*., 2020).

A study by Aki *et al*. (2004) discovered that anions were crucial in determining the solubility of CO_2. The study also denoted that fluoroalkyl-containing anions (such as [TFSI] and [methide]) presented higher solubilities than other anions. Likewise, Snuffin *et al*. (2011) reported that [EMIM][BF_3Cl] with a C_3 symmetric tetrahedral structure was more effective in electroreducing CO_2 compared to [BMIM][BF_4] and [BMIM][TFSI]. This outcome suggested a significant correlation between anion and catalytic performance. Nonetheless, insufficient studies have been observed regarding comprehending the precise reaction mechanisms and the distinct functions of cations and anions in electrochemical reduction reactions.

This study assessed the impact of different ILs on the CO_2 reduction peaks and current density values for two different CO_2ER setups. The molecular orbital energy levels [highest occupied molecular orbital (HOMO) and lowest occupied molecular orbital (LUMO)] of the various cations and anions were determined using a TmoleX simulation software. Furthermore, the impacts of the structure size and the HOMO value of the anion on the catalytic performance of CO_2 reduction were explored.

2. Materials and methods

2.1 Materials

The [BBT][BF_4], [BBT][TFSI], [BMIM][BF_4], and [BMIM][GLY] in this study were synthesised following the methods outlined in the authors' previous article (Mohammed *et al*., 2022). Meanwhile, [EMIM][TFSI] (purity: ≥97.0%) and [HMIM][TFSI] (purity: ≥98.0%) were obtained from Sigma Aldrich without requiring any further purification. Figure 1 illustrates the structures of the selected ILs for this study.

2.2 CO_2ER setup

The electroreduction was conducted in an H-cell, in which an Ag/AgCl electrode was used as the reference electrode, and a Pt mesh of (1 cm × 1 cm) area was employed as the anode in 0.5 M H_2SO_4 anolyte solution. A Nafion 117 membrane was also utilised to separate the catholyte and anolyte to prevent the re-oxidation of the reduction products. This membrane underwent pre-treatment through a series of three sequential steps: (i) pre-treatment using 3% hydrogen peroxide for 1 h at 80°C, (ii) pre-treatment using 0.5 M sulfuric acid solution for 1 h at 80°C, and (iii) rinsing process using distilled water. The purpose of this

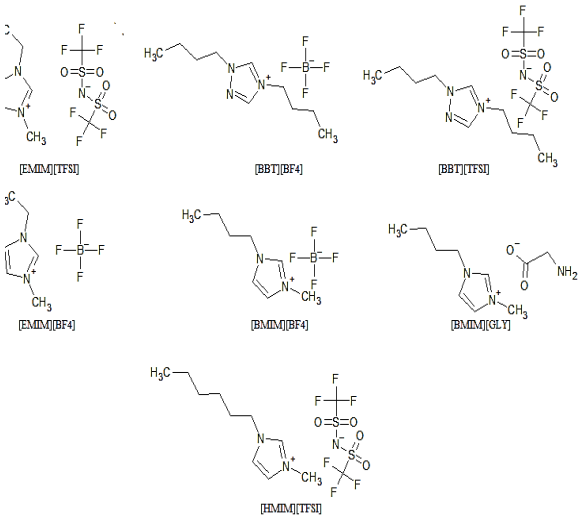

Figure 1. ILs structures used in this study.

procedure was to cleanse the membrane of organic contaminants and protonation of the membrane (Navarra *et al*., 2008). A 0.5 L gas bag was also attached to the catholyte side to collect the gaseous products. Meanwhile, various ILs were introduced as additives into two distinct electrolyte systems based on the solubility of the ILs: (i) 0.1 M $NaHCO_3$ aqueous solution and (ii) 0.1 M NBu_4PF_6 acetonitrile (ACN) solution.

A) CO_2ER in $NaHCO_3$-aqueous based electrolytes

Five different electrolytes were studied as the catholyte, namely 0.1 M $NaHCO_3$-based electrolytes containing 0.02 M of four different ILs, including [BBT][BF_4], [BMIM][GLY], I[EMIM][BF_4], and [BMIM][BF_4], alongside a 0.1 M $NaHCO_3$ solution without any IL. A copper (Cu) plate of 1 cm × 1 cm was used as the cathode, platinum (Pt) mesh as the anode, and Ag/AgCl as the reference electrode. The Cu plate was polished and cleaned using acetonitrile and water and then dried to eliminate particulate residue. Subsequently, N_2 gas was purged into the electrolytes for 15 mins. The pH of the selected electrolytes was then measured using a pH meter. Lastly, the electrolytes underwent a 40-minute purging process with CO_2, followed by an additional step of monitoring the pH before the CO_2ER reaction.

B) CO_2ER in NBu_4PF_6 -based electrolytes

The cathode utilised in this part was a silver disc electrode with a diameter of 2 mm. Seven different catholytes were prepared namely 0.1 M NBu_4PF_6 acetonitrile solutions containing 0.02 M of six ILs including BBT][BF_4], [BBT][TFSI], [EMIM][BF_4], [EMIM][TFSI], [BMIM][BF_4], and [HMIM][TFSI]. A 0.1 M NBu_4PF_6 ACN solution without any IL was also employed as a reference.

2.3 Evaluation of reduction peak and current density

The CO_2ER reaction was assessed using a potentiostat (AutoLAB, PGSTAT128N) equipped with NOVA software. This study then used linear sweep voltammetry (LSV) based on a scan rate of 0.0049 V/s to determine the CO_2 reduction peak. Finally, a chronoamperometry (CA) method was used to conduct the reaction, depending on the reduction peak potential.

DOI: https://doi.org/10.22452/mjs.vol43sp1.9
Malaysian Journal of Science 43 (Special Issue 1): 50-57 (July 2024)

2.4 Molecular computational modelling study

A molecular computer modelling investigation was conducted using TmoleX to optimise the chosen structures and determine the LUMO and HOMO values of these structures. The TmoleX programme utilised parametrisation, incorporating triple-zeta valence with polarisation (TZVP) based on density functional theory (DFT). Typically, the sigma profile and sigma potential present extensive uses in determining the polarity of the molecule (Khan *et al*., 2023; Khan *et al*., 2020; Wojeicchowski *et al*., 2021). Thus, these parameters were generated using COSMO-RS. The classifications of the parameters are as follows: (i) bond donor ($\sigma < -0.01$ e/Å^2), (ii) non-polar area for ($-0.01 < \sigma < +0.01$ e/Å^2), (iii) and hydrogen bond acceptor for ($\sigma > +0.01$ e/Å^2) (Klamt, 2005; Klamt, Jonas, Bürger, & Lohrenz, 1998).

3. Results and discussions

3.1 CO_2ER in 0.1 $NaHCO_3$ aqueous solution

Initially, the impact of introducing ILs on the pH of the CO_2ER system was evaluated. Table 1 tabulates the pH values for the selected electrolytes before and after purging CO_2, showing the pH reduction due to CO_2 absorption. Figure 2 illustrates the CO_2 reduction peaks for various electrolytes. These peaks were obtained using the LSV method to assess the correlation between the IL structure and the potential onset. Consequently, the potential onset followed a specific order beginning with the most favourable option: [EMIM][BF_4] > [BMIM][GLY] > [reference] > [BMIM][BF_4] > [BBT][BF_4].

Table 1. The pH values for the selected electrolytes before and after purging CO_2.

Electrolyte	pH (before CO_2 purging)	pH (after CO_2 purging)
Reference (0.1 $NaHCO_3$)	8.46	7.04
0.1 $NaHCO_3$ + 0.02M [EMIM][BF_4]	8.49	6.97
0.1 $NaHCO_3$ + 0.02M [BMIM][BF_4]	8.41	7.12
0.1 $NaHCO_3$ + 0.02M [BBT][BF_4]	8.49	7.11
0.1 $NaHCO_3$ + 0.02M [BMIM][GLY]	9.02	6.78

A study by Whipple *et al.* (2010) highlighted a negative correlation between pH value and concentration of protons (H^+) in the solution (lower pH = higher H^+), producing a higher CO_2 protonation. Given that the hydrogen evolution reaction (HER) rate competing with the CO_2 reduction reaction for electrons decreased, the production rates of the desired products were accelerated. On the contrary, this study presented that the sequence of pH values (starting from the lowest) did not align with the sequence of potential onsets (starting from the most positive) (see Table 1). Therefore, this outcome implied that no correlation between pH and onset reduction potential was observed. Meanwhile, Snuffin *et al.* (2011) explained that the catalytic reduction of CO_2 using IL salts was caused by the interaction between CO_2 and the anions of ILs, which was based on the Lewis acid-base mechanism.

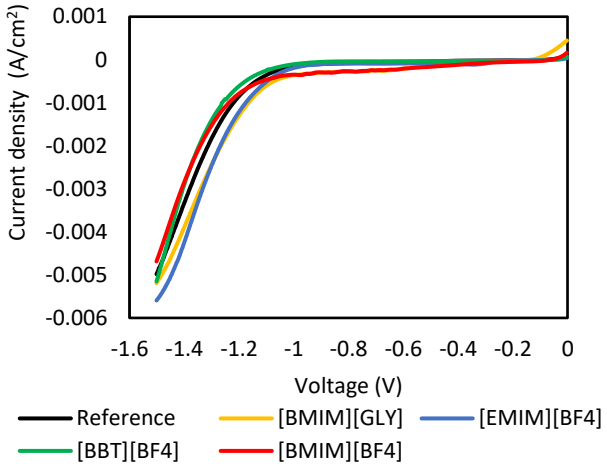

Figure 2. CO_2 reduction peaks for different 0.1 M 0.1 $NaHCO_3$

The CO_2ER reaction for the selected electrolytes was performed using CA for 2 h. Table 2 lists the applied potentials for the selected electrolytes and their corresponding current density values, as shown in Figure 3. Confirming Ohm's law, a higher applied potential resulted in higher current density. Moreover, the electrolyte containing the 0.1 M $NaHCO_3$ + 0.02 M EMIM BF_4 produced a lower applied potential and higher current density than the solution without IL. This finding was highly favourable for the CO_2ER system, in which the significantly higher current density was attributed to the enhanced conductivity arising from a higher concentration of ions in the solution. Therefore, this enhancement provided more charge carriers to facilitate the electric current conduction.

Nevertheless, a substantially lower current density at the same applied potential was observed for the 0.1 M $NaHCO_3$ + 0.02 M BMIM GLY electrolyte than the solution containing EMIM BF_4. This outcome could be explained by the strong interaction between glycinate ions and CO_2 through chemical absorption and extensive solvation, thus limiting the mobility of the ions and

Table 2. The applied potential for selected electrolytes and their corresponding current density

Electrolyte	Applied potential (V)	Current density (mA/cm^2)
Reference (0.1 $NaHCO_3$)	-1.42	-2.9
0.1 $NaHCO_3$ + 0.02M EMIM BF_4	-1.36	-3.8
0.1 NaHCO3 + 0.02M BMIM BF_4	-1.48	-4.9
0.1 $NaHCO_3$ + 0.02M BBT BF_4	-1.44	-4.84
0.1 $NaHCO_3$ + 0.02M BMIM GLY	-1.36	-2.77

DOI: https://doi.org/10.22452/mjs.vol43sp1.9
Malaysian Journal of Science 43 (Special Issue 1): 50-57 (July 2024)

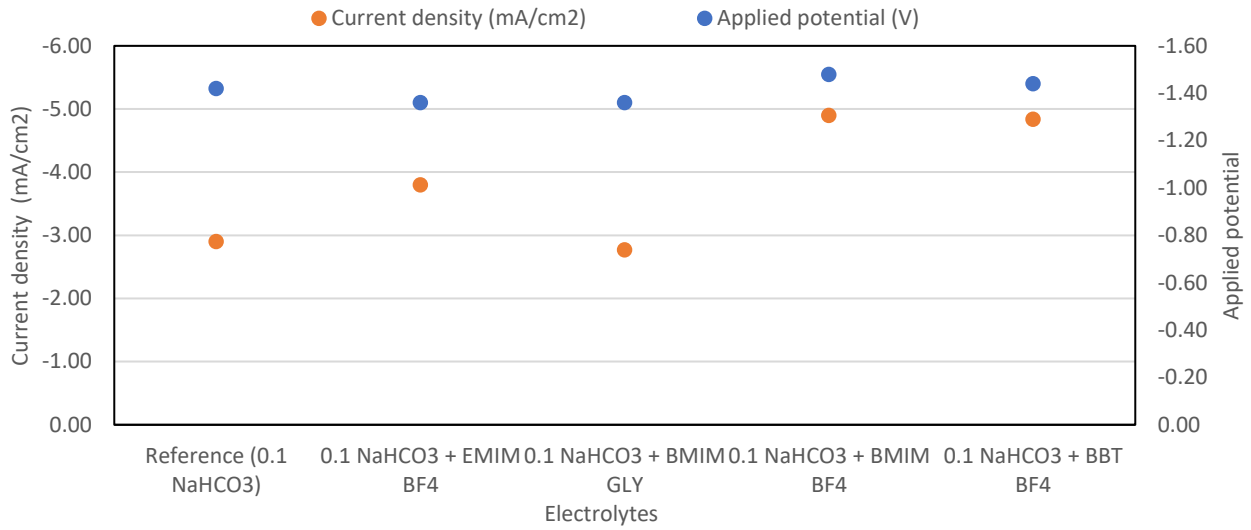

Figure 3: Chronoamperometry results for 0.1 $NaHCO_3$ aqueous electrolytes with and without ILs

decreasing current density (Mohammed *et al*., 2023). The same explanation could also describe the 0.1 M $NaHCO_3$ + 0.02 M BMIM GLY electrolyte demonstrating the lowest pH value. Nevertheless, this condition could be avoided by choosing an electrolyte with high basicity.

The alkyl chain length negatively impacted the transport parameters (conductivity and cation diffusion coefficients) (Every *et al*., 2004). Considering that the length of the alkyl chains in the cation increased, the packing density of the ions dropped, and the space between the cation and anion increased. This process weakened the ion-ion interactions and reduced the dissociation of the ions in the IL, causing a decrease in ionic conductivity. On the contrary, shorter alkyl chains resulted in a greater packing density of the ions and stronger ion-ion interactions, leading to improved ion dissociation and increased ionic conductivity.

3.2 CO_2 ER in 0.1 M NBu_4PF_6 ACN-Based solution

Figure 4 displays the CO_2 reduction peaks for different 0.1 M NBu_4PF_6 ACN-based electrolytes with and without ILs. The CO_2 reduction potential was lower in all electrolytes containing ILs than in the reference electrolyte. The [EMIM][BF_4] electrolyte solution exhibited a lower overpotential of 320 mV compared to the reference solution. Rosen *et al*. (2011) observed that [EMIM][BF_4] demonstrated a 96% faradaic efficiency on the silver cathode (Ag) and a significant capability to decrease the overpotential (approximately 200 mV higher than the equilibrium potential). Furthermore, the electrostatic interaction reduced when the alkyl chain length increased. This process reduced the transport characteristics, leading to more negative onset potential.

Table 3 summarises the results of the CA study at the applied potential and the corresponding current density value for each electrolyte after running the experiment for 30 minutes, with the corresponding graph in Figure 5. The ILs were observed to improve the current density, even at a lower potential than the reference electrolyte. This outcome was attributed to the higher mobility of IL ions compared to the larger structure of NBu_4PF_6.

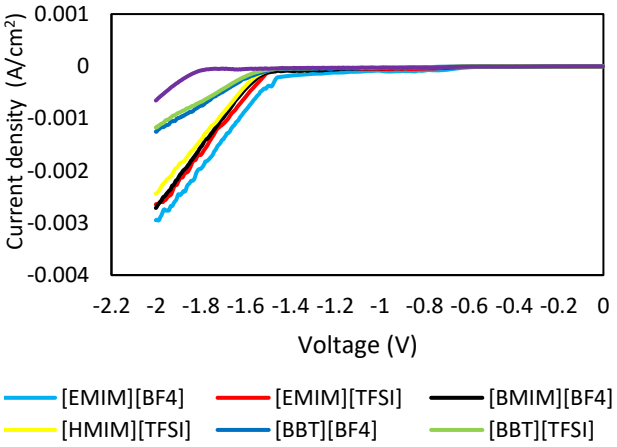

Figure 4: CO_2 reduction peaks in different 0.1 M NBu_4PF_6 acetonitrile-based electrolytes with and without ILs

Table 3. The applied potential for selected electrolytes and their corresponding current density

Electrolyte	Applied potential (V)	Current density (mA/cm²)
Reference (0.1 M NBu_4PF_6 in ACN)	-2.64	-3.40
0.1 M NBu_4PF_6 in ACN + 0.02M EMIM BF_4	-2.32	-4.40
0.1 M NBu_4PF_6 in ACN + 0.02M EMIM TFSI	-2.33	-4.60
0.1 M NBu_4PF_6 in ACN + 0.02M BMIM BF_4	-2.39	-4.40
0.1 M NBu_4PF_6 in ACN + 0.02M BBT BF_4	-2.42	-3.32
0.1 M NBu_4PF_6 in ACN + 0.02M BBT TFSI	-2.44	- 3.60
0.1 M NBu_4PF_6 in ACN + 0.02M HMIM TFSI	-2.34	-4.30

DOI: https://doi.org/10.22452/mjs.vol43sp1.9
Malaysian Journal of Science 43 (Special Issue 1): 50-57 (July 2024)

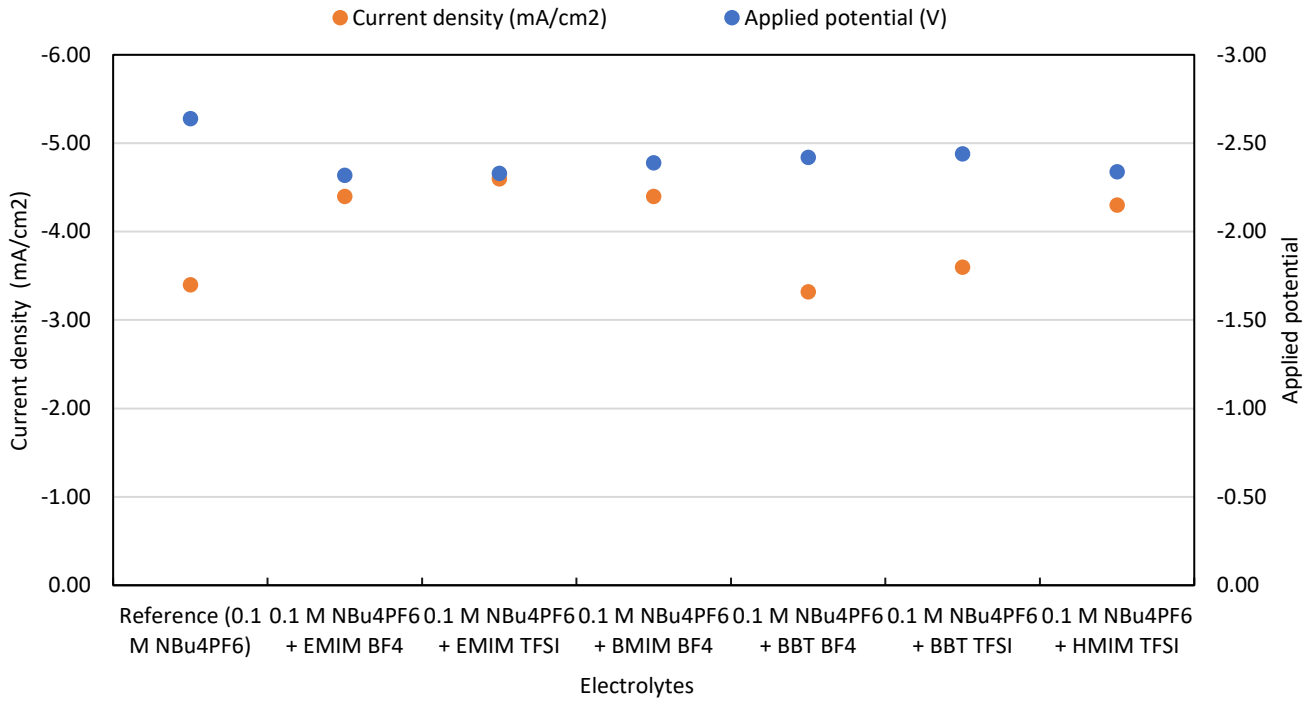

Figure 5: Chronoamperometry results for 0.1 M NBu_4PF_6 acetonitrile-based electrolytes with and without ILs

The applied potential for the same current density at 4.4 mA/cm^2 was also slightly higher for BMIM BF_4 with a longer alkyl chain when comparing the electrolytes containing EMIM BF_4. In addition, the influence of the alkyl chain was more pronounced for BBT BF_4. At a similar applied voltage, the BBT BF_4 exhibited significantly reduced current density compared to BMIM BF_4 due to the presence of the dibutyl chain on the triazolium ring. Thus, this outcome further confirmed that an increase in the alkyl chain length led to decreased ion mobility and increased resistance towards the electrode.

Further investigation of the effects of the IL structure on the molecular orbitals and CO_2ER was performed due to inadequate conclusive evidence. The frontier molecular orbital theory states that the interaction between a Lewis acid and a Lewis base occurs through the interaction of specific frontier orbitals of the acid and base (Fukui, 1975; Liu *et al*., 2020). This interaction involves the transfer of electrons from the HOMO level of the base to the LUMO level of the acid. Therefore, the impact of molecular orbital levels on CO_2 reduction potential is highly relevant. Figure 6 portrays the HOMO and LUMO values of [EMIM], [BMIM], [BBT], [BF_4], [TFSI], and [GLY] calculated using TmoleX.

A significantly higher HOMO value was observed for the [GLY] anion than the [BF_4] anion. Even though the [GLY] anion also demonstrated a notably lower current density than the [BMIM][BF_4], a more favourable onset potential was presented (see Figure 3). Given that CO_2 was the Lewis acid and anions were the Lewis base, anions with higher HOMO values possessed a more significant positive reduction potential. A study by Gomes *et al*. (2022) also highlighted that the [TFSI] anion produced a decreased capability for reducing CO_2 compared to [BF_4]. Typically, the [TFSI] anion exhibits a greater HOMO value in comparison to [BF_4]. Therefore, the anions with higher HOMO values improved the efficiency of CO_2ER by reducing the overpotential. Nonetheless, a significant pH decrease was observed for a strong acid or base interaction between the anion and CO_2 (such as glycinate), which produced a detrimental effect on reducing the current density.

Another study by Monteiro *et al*. (2021) presented three main hypotheses on the impact of cations on the activity and selectivity of electrocatalytic processes at the interface. These hypotheses suggested that the cations modified the local electric field, buffer the interfacial pH, or stabilise reaction intermediates. The study also explained that cation acidity substantially impacted the CO_2ER, which acidic cations promoted CO_2ER at low overpotentials and in acidic media. Meanwhile, Lau et al. (2016) described that the acidic proton at the C_2 position of the

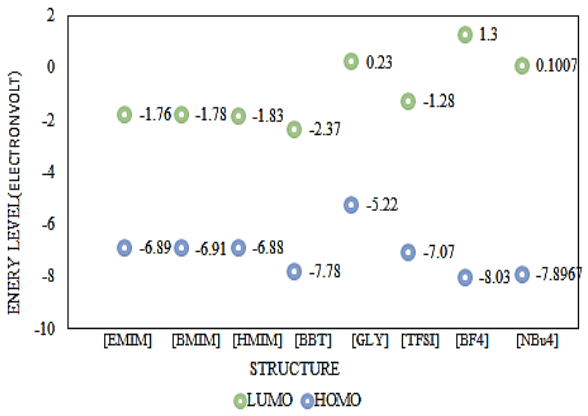

Figure 6. LUMO and HOMO values for the selected structures.

DOI: https://doi.org/10.22452/mjs.vol43sp1.9
Malaysian Journal of Science 43 (Special Issue 1): 50-57 (July 2024)

imidazolium ring stabilised the intermediate CO_2 anion radical by forming hydrogen bonds, which rendered it a significant catalytic site. Similarly, Neyrizi *et al*. (2022) concluded a direct correlation between the performance of CO_2 reduction and acidity of the imidazolium cation (C_2-H).

This study investigated the cation effect on CO_2ER by examining the CO_2 reduction for the same anion. Figure 2 illustrates that for the same anion, the order of CO_2 reduction for [BF_4] (starting from the more positive onset potential) was [EMIM][BF_4] > [BMIM][BF_4] > [BBT][BF_4]. In contrast, the sequence of cation acidity did not follow a similar trend as the CO_2 reduction overpotential, in which the order of LUMO values of the cations (starting from the lowest) was [BBT] < [BMIM] < [EMIM]. Our previous study deduced that a low LUMO value of the cation (acidity) enhanced the solubility of CO_2 by facilitating an acid/base interaction between the cation and the negatively charged oxygen (Mohammed *et al*., 2023). Therefore, a long cation alkyl chain could present difficulties reaching the electrode surface, impeding its proximity with the electrons. This observation was attributed to the positively charged nitrogen atom of the cation that was relatively far from the electrode surface due to the long alkyl chain.

Coulomb's law states that the electrostatic attraction or repulsion intensity between two-point charges is directly proportional to the product of their magnitudes and inversely proportional to the square of the distance between them. A study by Azra *et al*. (2022) supported this statement by demonstrating the correlation between long alkyl chains and molecular interaction. The study highlighted the significance of chain length in separating organic and aqueous phases, in which longer chain lengths promoted easy separation. In contrast, shorter chain lengths enhanced water clarity, hindering complete separation and resulting in lower extraction efficiency. Considering that the disparity in the LUMO values between the cations was not substantial, the long alkyl chain of a cation decreased the interaction between its positively charged nitrogen and the electrons on the electrode to a greater extent than the magnitude of the charge. When an electric potential was provided, the positively charged ions migrated towards the negatively charged electrode (cathode). Consequently, the long non-polar alkyl chain decreased or increased the mobility of the ions or resistance towards the electrode, respectively.

Figure 5 demonstrates that the inclusion of ILs significantly improves the system. This observation was due to the inclusion of ILs enhancing the acid or base interaction with CO_2. Additionally, a higher non-polar/non-polar interaction with CO_2 and lower acid/base interaction was observed owing to the large structure and the long alkyl chain of NBu_4PF_6. Figure 7 depicts the sigma profile and sigma potential of the cations and anions. Similar to CO_2, the NBu_4PF_6 was highly non-polar. Overall, the CO_2 exhibited a dual nature, with both partially charged properties that allowed it to interact with its environment through acid/base interaction and non-polar characteristics (due to the linear structure of its bonds). Thus, the CO_2ER was greatly affected by the interaction between CO_2 and the electrolyte environment.

Another study by Ueno *et al*. (2010) denoted that the solvation of strongly Lewis basic anions and highly Lewis acidic cations by solvents enabled a substantial level of salt dissociation. Therefore, selecting a favourable combination of ILs with a short alkyl chain, an anion with a high HOMO value, and a compatible

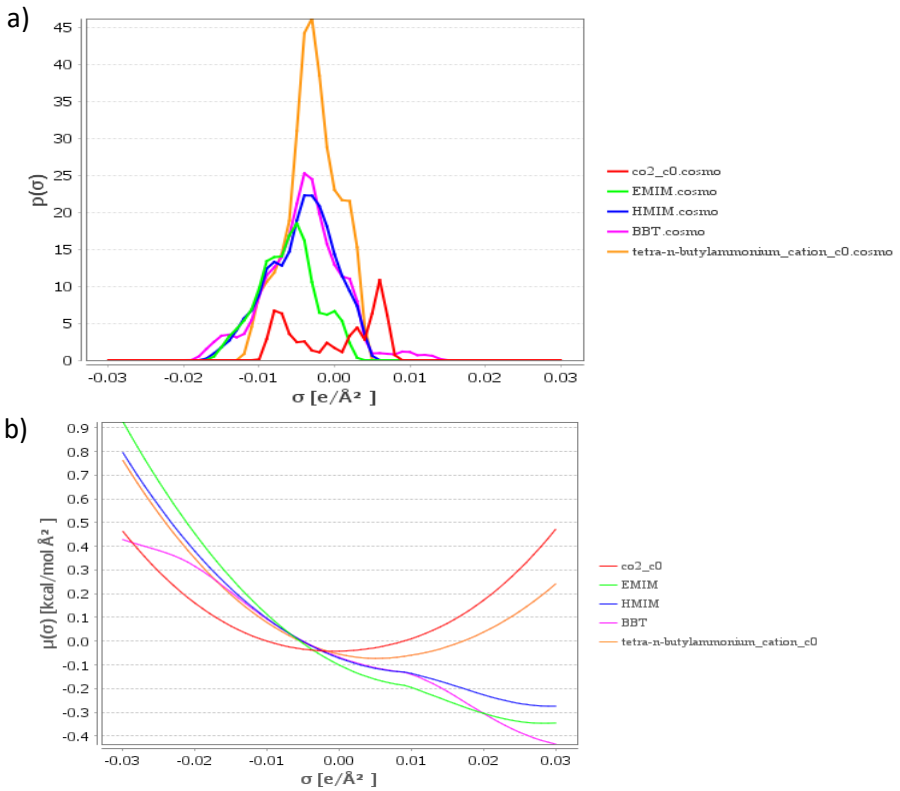

Figure 7: Sigma profile (a) and sigma potential (b) of the cations and anions of ILs including CO_2

DOI: https://doi.org/10.22452/mjs.vol43sp1.9
Malaysian Journal of Science 43 (Special Issue 1): 50-57 (July 2024)

solvent increased the current density. The performance of the CO_2ER system was also reduced when the non-polar/non-polar interaction between the ILs and CO_2 was dominant. Thus, cations with short alkyl chains and anions with high HOMO values were essential to improve the acid/base interaction between CO_2 and electrolytes for optimal performance of ILs in CO_2ER. Notably, cations with short alkyl chains lowered the resistance to charge resistance at the electrode.

4. Conclusion

In this study, The CO_2 reduction peaks, and the current density of different electrolytes were evaluated using linear sweep voltammetry (LSV), and chronoamperometry (CA). HPLC and GC-TCD were used to confirm the formation of the reaction products. The addition of 1-ethyl-3-methylimidazolium tetrafluoroborate [EMIM][BF_4] to the 0.1 M NBu_4PF_6 acetonitrile solution demonstrates that the reduction's onset potential significantly decreased by 320 mV. It can be concluded that to have effective ionic liquid as electrolyte for CO_2ER reaction, in order to have low overpotential and high current density, the acid/base interaction with IL and CO_2 is desirable , and for that ILs with small alkyl chain, low LUMO values of cations and high HOMO values as anions are recommended while considering the suitable organic solvent.

5. Acknowledgement

The Fundamental Research Grant Scheme initiative of the Malaysian Ministry of Higher Education provided funding for this study (MOHE-FRGS/1/2021/TK0/UTP/02/12). Additionally, the authors acknowledge the Chemical Engineering Department, the Centre for Research in Ionic Liquids (CORIL), the Centre for Biofuel and Biochemical Research (CBBR), and Centre for Corrosion Research (CCR) of Universiti Teknologi PETRONAS (UTP) for their technical assistance and resources.

6. References

Aki, S. N., Mellein, B. R., Saurer, E. M., & Brennecke, J. F. (2004). High-pressure phase behavior of carbon dioxide with imidazolium-based ionic liquids. *The Journal of Physical Chemistry B, 108*(52), 20355-20365.

Azra, N., Nazir, F., Roosh, M., Khalid, M. A., Mansoor, M. A., Khan, S. B., & Iqbal, M. (2022). Extraction of Pb (II) and Co (II) using N, N-dioctylsuccinamate based room temperature ionic liquids containing aliphatic and aromatic cations. Arabian Journal of Chemistry, 15(9), 104099.

Bi, Z.x., Guo, R.t., Hu, X., Wang, J., Chen, X., & Pan, W.g. (2022). Research progress on photocatalytic reduction of CO_2 based on LDH materials. *Nanoscale, 14*(9), 3367-3386.

Carlesi, C., Carvajal, D., Vasquez, D., & Arratia, R. S. (2014). Analysis of carbon dioxide-to-methanol direct electrochemical conversion mediated by an ionic liquid. *Chemical Engineering Processing: Process Intensification 85*, 48-56.

Every, H. A., Bishop, A. G., MacFarlane, D. R., Orädd, G., & Forsyth, M. (2004). Transport properties in a family of dialkylimidazolium ionic liquids. *Physical Chemistry Chemical Physics, 6*(8), 1758-1765.

Friedlingstein, P., Andrew, R. M., Rogelj, J., Peters, G. P., Canadell, J. G., Knutti, R., . van Vuuren, D. P. (2014). Persistent growth of CO_2 emissions and implications for reaching climate targets. *Nature geoscience, 7*(10), 709-715.

Fukui, K. (1975). *Theory of Orientation*: Springer.

Gu, J., Liu, S., Ni, W., Ren, W., Haussener, S., & Hu, X. (2022). Modulating electric field distribution by alkali cations for CO_2 electroreduction in strongly acidic medium. *Nature Catalysis, 5*(4), 268-276.

Hori, Y., Murata, A., Kikuchi, K., & Suzuki, S. (1987). Electrochemical reduction of carbon dioxides to carbon monoxide at a gold electrode in aqueous potassium hydrogen carbonate. *Journal of the Chemical Society, Chemical Communications*, 728-729.

Hori, Y., Wakebe, H., Tsukamoto, T., & Koga, O. (1994). Electrocatalytic process of CO selectivity in electrochemical reduction of CO_2 at metal electrodes in aqueous media. *Electrochimica Acta, 39*(11-12), 1833-1839.

Hori, Y.,(2008). Electrochemical CO_2 reduction on metal electrodes. In *Modern aspects of electrochemistry* (pp. 89-189): Springer.

Khan, H. W., Khan, M. K., Moniruzzaman, M., Al Mesfer, M. K., Danish, M., Irshad, K., . Chelliapan, S. (2023). Evaluating ionic liquids for its potential as eco-friendly solvents for naproxen removal from water sources using COSMO-RS: Computational and experimental validation. *Environmental Research*, 116058.

Khan, H. W., Reddy, A. V. B., Nasef, M. M. E., Bustam, M. A., Goto, M., & Moniruzzaman, M. (2020). Screening of ionic liquids for the extraction of biologically active compounds using emulsion liquid membrane: COSMO-RS prediction and experiments. *J. Mol. Liq., 309*, 113122.

Klamt, A. (2005). *COSMO-RS: from quantum chemistry to fluid phase thermodynamics and drug design*. Germany: Elsevier.

Klamt, A., Jonas, V., Bürger, T., & Lohrenz, J. C. (1998). Refinement and parametrization of COSMO-RS. *J. Phys. Chem A, 102*(26), 5074-5085.

Lau, G. P., Schreier, M., Vasilyev, D., Scopelliti, R., Grätzel, M., & Dyson, P. J. (2016). New insights into the role of imidazolium-based promoters for the electroreduction of CO_2 on a silver electrode. *Journal of the American Chemical Society, 138*(25), 7820-7823.

Lau, G. P. S., Schreier, M., Vasilyev, D., Scopelliti, R., Grätzel, M., & Dyson, P. J. (2016). New Insights into the Role of Imidazolium-Based Promoters for the Electroreduction of CO_2 on a Silver Electrode. *Journal of the American Chemical Society, 138*, 7820-7823.

DOI: https://doi.org/10.22452/mjs.vol43sp1.9
Malaysian Journal of Science 43 (Special Issue 1): 50-57 (July 2024)

Liu, C., Li, Y., Takao, M., Toyao, T., Maeno, Z., Kamachi, T., . . . Shimizu, K.i. (2020). Frontier molecular orbital based analysis of solid–adsorbate interactions over group 13 metal oxide surfaces. *The Journal of Physical Chemistry C 124*(28), 15355-15365.

Mohammed, S. A. S., Yahya, W. Z. N., Bustam, M. A., & Kibria, M. G. (2023). Experimental and Computational Evaluation of 1, 2, 4-Triazolium-Based Ionic Liquids for Carbon Dioxide Capture. *Separations, 10*(3), 192.

Mohammed, S. A. S., Yahya, W. Z. N., Bustam, M. A., Kibria, M. G., Masri, A. N., & Kamonwel, N. D. M. (2022). Study of the ionic liquids' electrochemical reduction using experimental and computational methods. *Journal of Molecular Liquids*, 119219.

Monteiro, M. C., Dattila, F., Hagedoorn, B., García-Muelas, R., López, N., & Koper, M. T. (2021). Absence of CO_2 electroreduction on copper, gold and silver electrodes without metal cations in solution. *Nature Catalysis, 4*(8), 654-662.

Navarra, M., Abbati, C., & Scrosati, B. (2008). Properties and fuel cell performance of a Nafion-based, sulfated zirconia-added, composite membrane. *Journal of power sources, 183*(1), 109-113.

Neyrizi, S., Kiewiet, J., Hempenius, M. A., & Mul, G. (2022). What It Takes for Imidazolium Cations to Promote Electrochemical Reduction of CO_2. *ACS Energy Letters, 7*(10), 3439-3446.

Rosen, B. A., Haan, J. L., Mukherjee, P., Braunschweig, B., Zhu, W., Salehi-Khojin, A., . Masel, R. I. (2012). In situ spectroscopic examination of a low overpotential pathway for carbon dioxide conversion to carbon monoxide. *Journal of Physical Chemistry C, 116*, 15307-15312.

Rosen, B. A., Salehi-Khojin, A., Thorson, M. R., Zhu, W., Whipple, D. T., Kenis, P. J. A., & Masel, R. I. (2011). Ionic liquid-mediated selective conversion of CO_2 to CO at low overpotentials. *Science, 334*, 643-644.

Shi, Z., Yang, H., Gao, P., Chen, X., Liu, H., Zhong, L., . Sun, Y. (2018). Effect of alkali metals on the performance of CoCu/TiO2 catalysts for CO2 hydrogenation to long-chain hydrocarbons. *Chinese Journal of Catalysis, 39*(8), 1294-1302.

Snuffin, L. L., Whaley, L. W., & Yu, L. (2011). Catalytic electrochemical reduction of CO_2 in ionic liquid $EMIMBF_3Cl$. *Journal of The Electrochemical Society, 158*, 155-158.

Tian, J., Yu, L., Xue, R., Zhuang, S., & Shan, Y. (2022). Global low-carbon energy transition in the post-COVID-19 era. *Applied energy 307*, 118205.

Ueno, K., Tokuda, H., & Watanabe, M. (2010). Ionicity in ionic liquids: correlation with ionic structure and physicochemical properties. *Physical Chemistry Chemical Physics, 12*(8), 1649-1658.

Vasilyev, D. V., Shyshkanov, S., Shirzadi, E., Katsyuba, S. A., Nazeeruddin, M. K., & Dyson, P. J. (2020). Principal descriptors of ionic liquid co-catalysts for the electrochemical reduction of CO_2. *ACS Applied Energy Materials, 3*(5), 4690-4698.

Whipple, D. T., Finke, E. C., & Kenis, P. J. (2010). Microfluidic reactor for the electrochemical reduction of carbon dioxide: the effect of pH. *Electrochemical Solid-State Letters, 13*(9), B109.

Wojeicchowski, J. P., Abranches, D. O., Ferreira, A. M., Mafra, M. R., Coutinho, J. o. A., & Engineering. (2021). Using COSMO-RS to Predict Solvatochromic Parameters for Deep Eutectic Solvents. *ACS Sustainable Chemistry, 9*(30), 10240-10249.

Yang, H., Xu, Z., Fan, M., Gupta, R., Slimane, R. B., Bland, A. E., & Wright, I. (2008). Progress in carbon dioxide separation and capture: A review. *Journal of environmental sciences, 20*(1), 14-27.

DOI: https://doi.org/10.22452/mjs.vol43sp1.9
Malaysian Journal of Science 43 (Special Issue 1): 50-57 (July 2024)